Supporting Information

Scalable engineering of hierarchical layered micro-sized silicon/graphene hybrids via direct foaming for lithium storage

Mathar Hamza,‡[a,b] Siyuan Zhang,‡[a,b] Wenqiang Xu,[a] Denghui Wang,[a,b] Yingjie Ma,[a,*] Xianglong Li [a,b,*]

[a] CAS Key Laboratory of Nanosystem and Hierarchical Fabrication, CAS Center for Excellence in Nanoscience, National Center for Nanoscience and Technology, Beijing 100190, P.R. China. a. Email: lixl@nanoctr.cn, mayj@nanoctr.cn

[b] University of Chinese Academy of Sciences, Beijing 100039, P.R. China.

‡ Mathar Hamza and Siyuan Zhang contributed equally to this work.

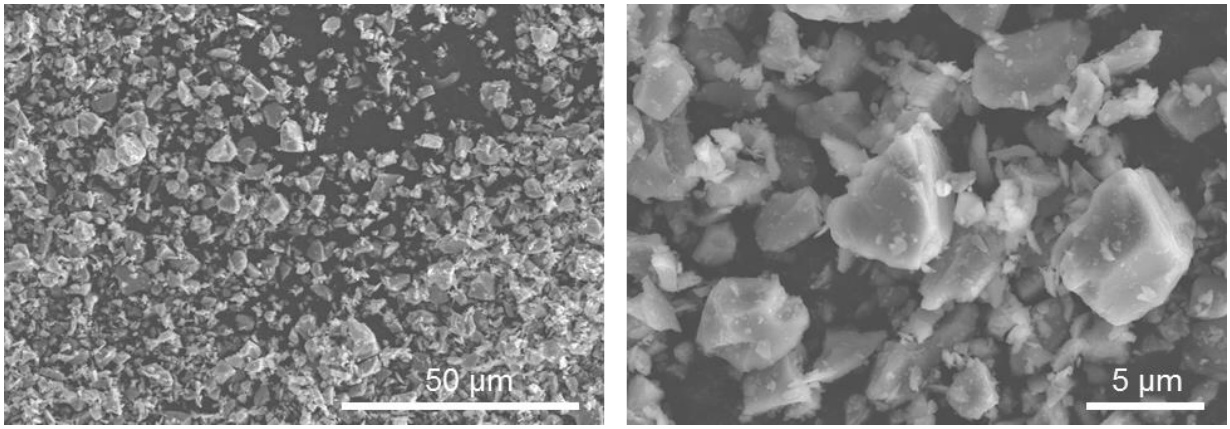

Fig. S1 SEM images of micro-sized Si.

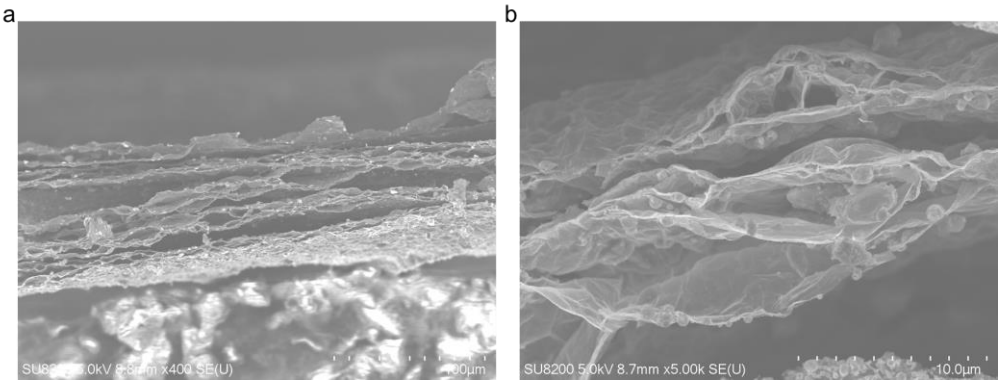

Fig. S2 SEM images of f-G-Si.

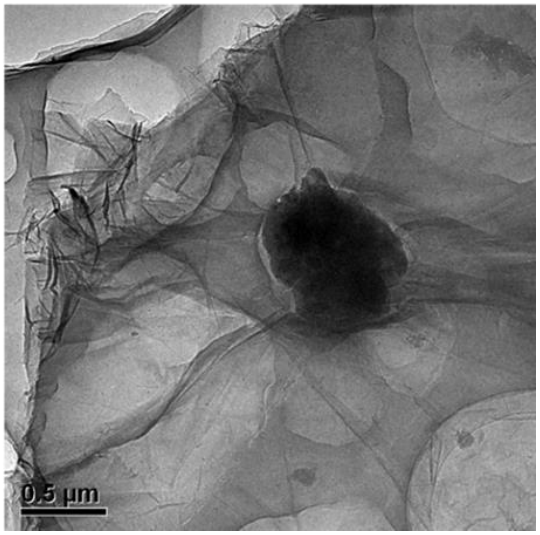

Fig. S3 The TEM image of G-Si

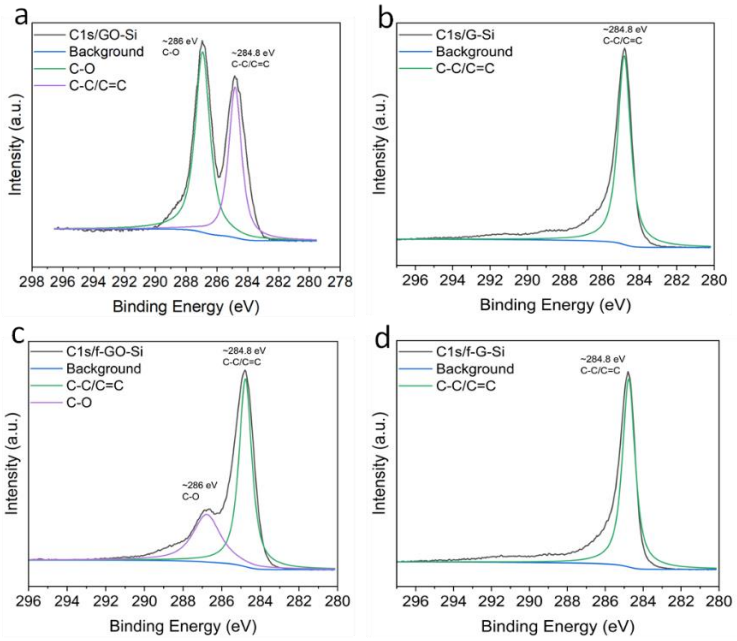

Fig. S4 C1s spectra of (a) GO-Si, (b) G-Si, (c) f-GO-Si, and (d) f-G-Si

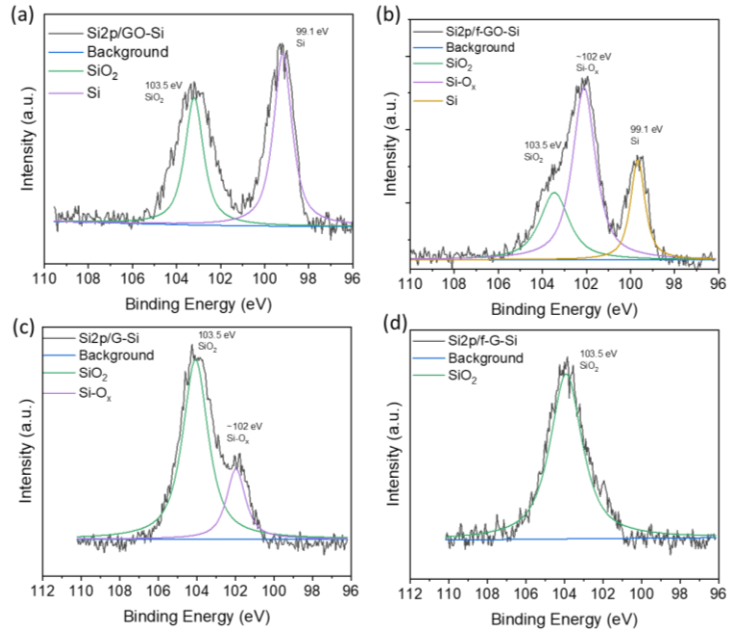

Fig. S5 Si2p XPS spectra of (a) GO-Si, (b) f-GO-Si, (c) G-Si, and (d) f-G-Si.

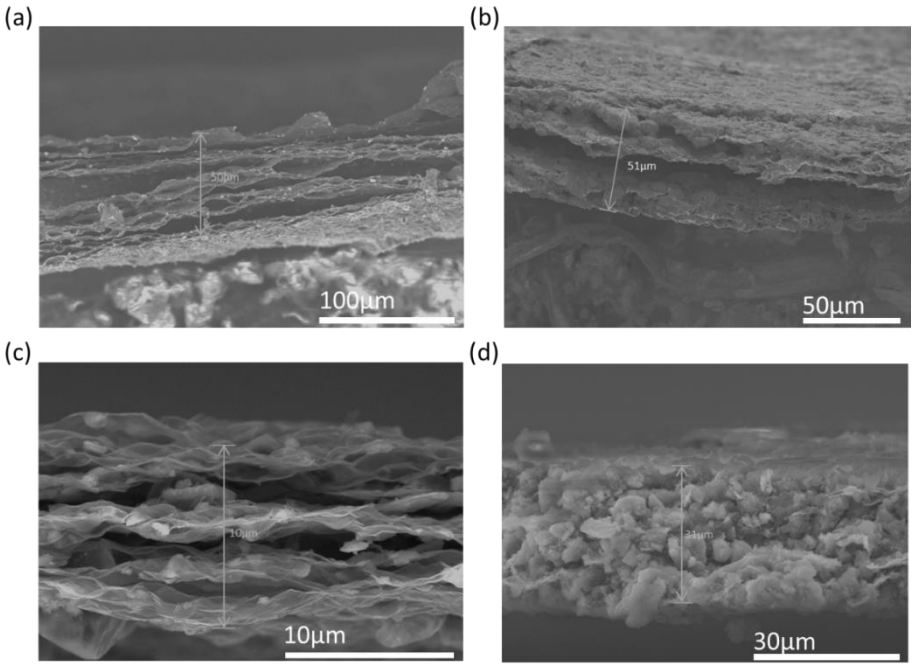

Fig. S6 SEM images of cross section of (a,b) f-G-Si and (c,d) G-Si after long cycling up to 500 cycles at 1 Ag^{-1}.

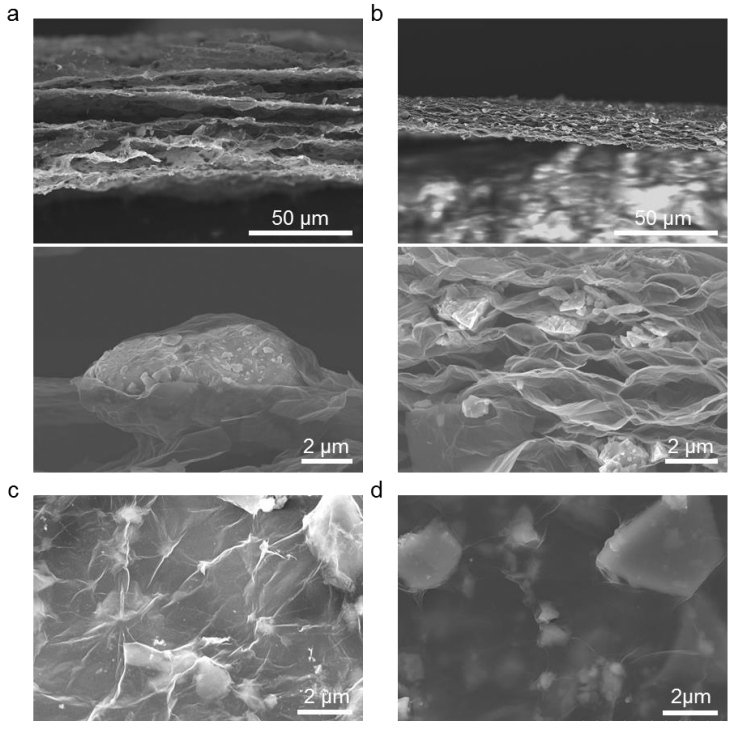

Fig. S7 SEM images of (a) and (c) f-G-Si, and (b) and (d) G-Si with lower silicon content (52% silicon).

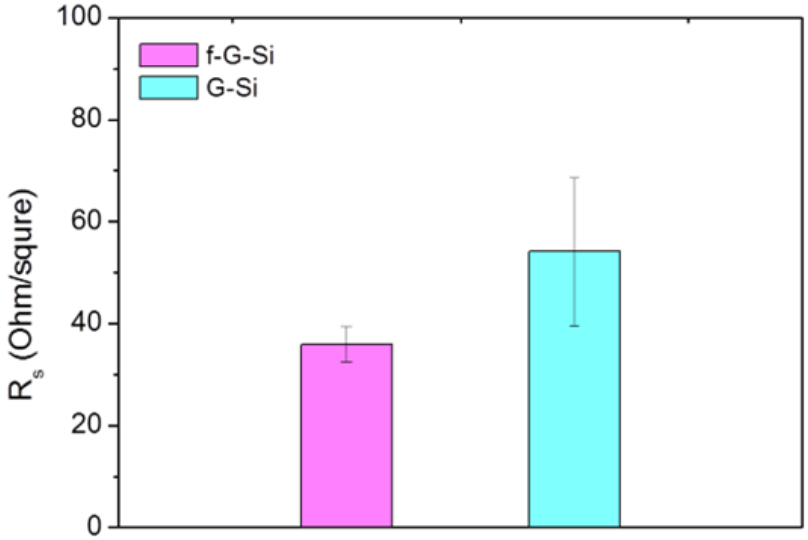

Fig. S8 Sheet resistance characteristics of f-G-Si and G-Si.

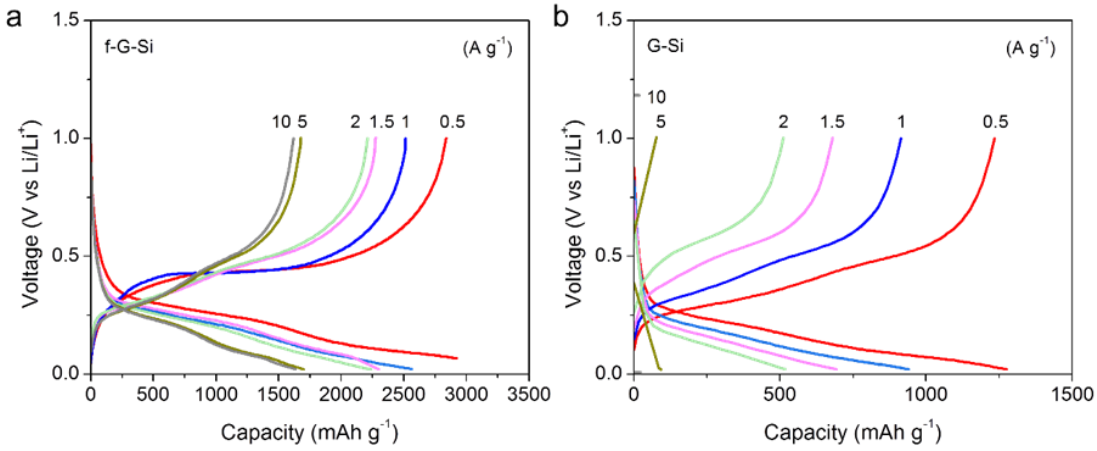

Fig. S9 Discharge-charge profiles of (a) f-G-Si and (b) G-Si at different current densities.

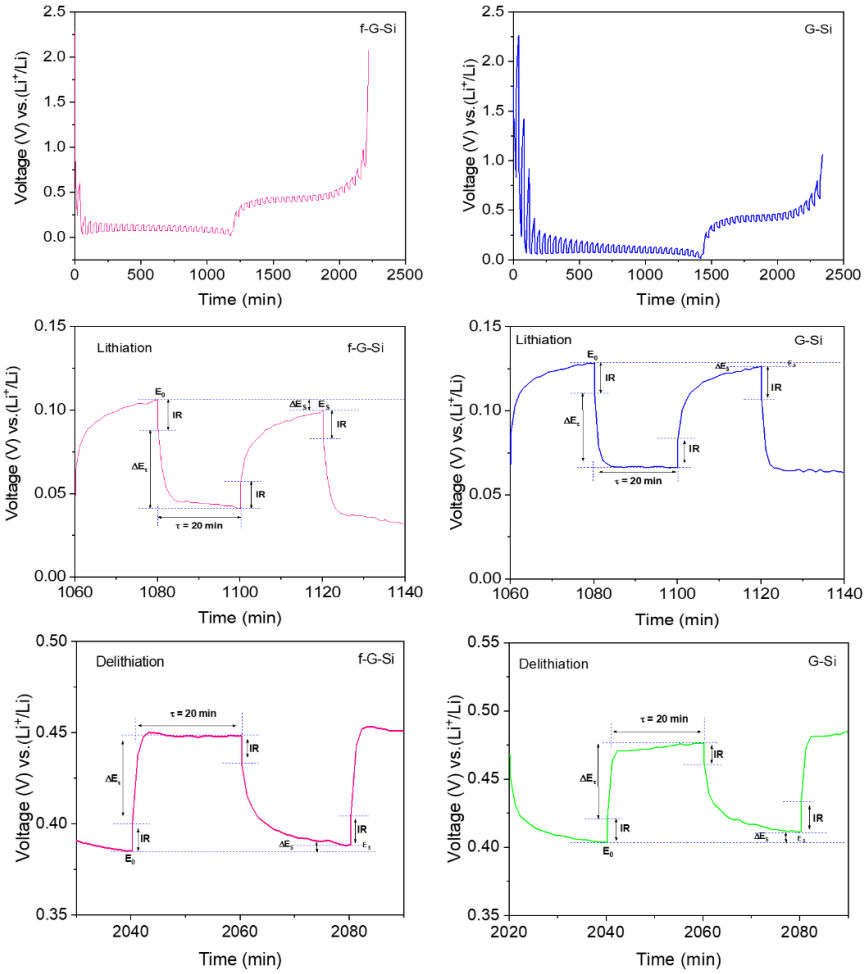

Fig. S10 GITT curves of (a) f-G-Si and (b) G-Si.

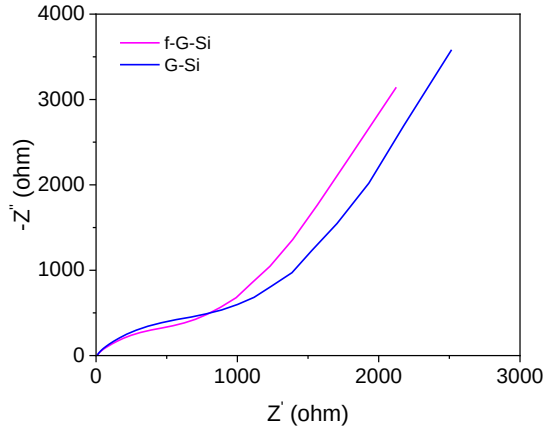

Fig. S11 Nyquist plots of f-G-Si and G-Si.

Table S1a. BET surface area &Pore size distribution of G-Si

BET Surface Area:	1.3706 m^2/g
Pore Width (nm)	Cumulative Pore Volume (cm^3/g)
1.483289338	0.000364355
1.590515054	0.000364355
1.715611708	0.000364355
1.8585793	0.000364355
2.001546978	0.000364355
2.16238568	0.000364355

Table S1b. BET surface area &Pore size distribution of f-G-Si

BET Surface Area:	**3.7614 m^2/g**
Pore Width (nm)	**Cumulative Pore Volume (cm^3/g)**
1.483289	0.000805
1.590515	0.000805
1.715612	0.000805
1.858579	0.000805
2.001547	0.000805
2.162386	0.000805
2.341095	0.000805
2.519805	0.000805

Table S2. The electrochemical performance comparison between previously reported graphene/silicon hybrid anodes and f-G-Si

Materials	Capacity	Cycles	Current density	References
Freeze drying Si nanoparticles with Graphene	1248.8 mAh g^{-1}	100	1200 mA g^{-1}	[1]
Si NS + rGO, LBL filtration	2030 mAh g^{-1}	150	200 mA g^{-1}	[2]
Si NP + GO, co-filtration	1650 mAh g^{-1}	100	100 mA g^{-1}	[3]
Silicon/graphene composite using solvent exchange method	~1500 mAh g^{-1}	30	200 mA g^{-1}	[4]
Watermelon-inspired Si/C microspheres	650 mAh g^{-1}	250	325 mA g^{-1}	[5]
sm-Si@C/Gr (<~1 µm)	1192 mAh g^{-1}	100	1000 mA g^{-1}	[6]
Si-based gel	1085.3 mAh g^{-1}	100	420 mA g^{-1}	[7]
P-doped Si 0.1-1 µm	587.7 mAh g^{-1}	50	200 mA g^{-1}	[8]
SiMP/SHP/CB ~3-8 µm	2093.6 mAh g^{-1}	90	400 mA g^{-1}	[9]
SiMP@Gr ~1-3 µm	~1260 mAh g^{-1}	300	2100 mA g^{-1}	[10]
PR-PAA–SiMP ~2.1 µm	2271 mAh g^{-1}	150	667 mA g^{-1}	[11]
Micro-sized Si/C 1-2 µm	1860 mAh g^{-1}	60	100 mA g^{-1}	[12]
mSi@OG@RGO (~1-5 µm)	1750 mAh g^{-1}	150	2000 mA g^{-1}	[13]
f-G-Si (~1-5 µm)	**1334 mAh g^{-1}**	**200**	**1000 mA g^{-1}**	**This work**

References

1. V. Chabot, K. Feng, H. W. Park, F. M. Hassan, A. R. Elsayed, A. Yu, X. Xiao and Z. Chen, Graphene wrapped silicon nanocomposites for enhanced electrochemical performance in lithium ion batteries, *Electrochim. Acta*, 2014, **130**, 127-134.

2. H. Zhang, S. Jing, Y. Hu, H. Jiang and C. Li, A flexible freestanding Si/rGO hybrid film anode for stable Li-ion batteries, *J. Power Sources.*, 2016, **307**, 214-219.

3. H. Jiang, X. Zhou, G. Liu, Y. Zhou, H. Ye, Y. Liu and K. Han, Free-standing Si/graphene paper using Si nanoparticles synthesized by acid-etching Al-Si alloy powder for high-stability Li-ion battery anodes, *Electrochim. Acta*, 2016, **188**, 777-784.

4. D. P. Wong, H.-P. Tseng, Y.-T. Chen, B.-J. Hwang, L.-C. Chen and K.-H. Chen, A stable silicon/graphene composite using solvent exchange method as anode material for lithium ion batteries, *Carbon*, 2013, **63**, 397-403.

5. Q. Xu, J. Y. Li, J. K. Sun, Y. X. Yin, L. J. Wan and Y. G. Guo, Watermelon-inspired Si/C microspheres with hierarchical buffer structures for densely compacted lithium-ion battery anodes, *Adv. Energy Mater.*, 2017, **7**, 1601481.

6. B. Lee, T. Liu, S. K. Kim, H. Chang, K. Eom, L. Xie, S. Chen, H. D. Jang and S. W. Lee, Submicron silicon encapsulated with graphene and carbon as a scalable anode for lithium-ion batteries, *Carbon*, 2017, **119**, 438-445.

7. F. Lyu, Z. Sun, B. Nan, S. Yu, L. Cao, M. Yang, M. Li, W. Wang, S. Wu and S. Zeng, Low-cost and novel Si-based gel for Li-ion batteries, *ACS Appl. Mater. Interfaces.*, 2017, **9**, 10699-10707.

8. S. Huang, L.-Z. Cheong, D. Wang and C. Shen, Nanostructured phosphorus doped silicon/graphite composite as anode for high-performance lithium-ion batteries, *ACS Appl. Mater. Interfaces.*, 2017, **9**, 23672-23678.

9. C. Wang, H. Wu, Z. Chen, M. T. McDowell, Y. Cui and Z. Bao, Self-healing chemistry enables the stable operation of silicon microparticle anodes for high-energy lithium-ion batteries, *Nat. chem.*, 2013, **5**, 1042-1048.

10. Y. Li, K. Yan, H.-W. Lee, Z. Lu, N. Liu and Y. Cui, Growth of conformal graphene cages on micrometre-sized silicon particles as stable battery anodes, *Nat. Energy*, 2016, **1**, 1-9.

11. S. Choi, T.-w. Kwon, A. Coskun and J. W. Choi, Highly elastic binders integrating polyrotaxanes for silicon microparticle anodes in lithium ion batteries, *Science*, 2017, **357**, 279-283.

12. D. Wang, M. Gao, H. Pan, Y. Liu, J. Wang, S. Li and H. Ge, Enhanced cycle stability of micro-sized Si/C anode material with low carbon content fabricated via spray drying and in situ carbonization, *J.Alloys. Compod*, 2014, **604**, 130-136.

13. X. Zhang, R. Guo, X. Li and L. Zhi, Scallop-Inspired Shell Engineering of Microparticles for Stable and High Volumetric Capacity Battery Anodes, *Small*, 2018, **14**, 1800752.